Compensating Pulse Imperfections in Solid-State NMR Spectroscopy: A Key to Better Reproducibility and Performance

Johannes J. Wittmann, Kazuyuki Takeda, Beat H. Meier,* and Matthias Ernst*

Abstract: The power and versatility of NMR spectroscopy is strongly related to the ability to manipulate NMR interactions by the application of radio-frequency (rf) pulse sequences. Unfortunately, the rf fields seen by the spins differ from the ones programmed by the experimentalist. Pulse transients, i.e., deviations of the amplitude and phase of the rf fields from the desired values, can have a severe impact on the performance of pulse sequences and can lead to inconsistent results. Here, we demonstrate how transient-compensated pulses can greatly improve the efficiency and reproducibility of NMR experiments. The implementation is based on a measurement of the characteristics of the resonance circuit and does not rely on an experimental optimization of the NMR signal. We show how the pulse sequence has to be modified to use it with transient-compensated pulses. The efficiency and reproducibility of the transient-compensated sequence is greatly superior to the original POST-C7 sequence.

$\mathbf{N}$MR pulse sequences consist of radio-frequency pulses with defined amplitude and phase acting on the spins. A simple example are rectangular "hard" pulses usually assumed to have an infinitely short rising and falling time and constant phase (Figure 1 A). In reality, however, the actual rf field experienced by the nuclear spins inside a tuned coil deviates significantly from the intended profile[1,2] as shown in Figure 1 B. Besides a delayed build-up and decay of the in-phase rf-field amplitude, also out-of-phase contributions are observed at the beginning and end of the pulse, referred to as pulse transients.[1,3–6] These imperfections impact the performance of the pulse sequences, especially if the spin interaction to be exploited in the experiment (e.g. the dipolar interactions) is small compared to potentially competing error terms. Therefore, a reduced sensitivity to phase transients is indeed a design principle for robust pulse sequences.[6] While phase transients were experimentally minimized on spectrometers with tube amplifiers[7–10] by tuning and matching the amplifier, modern NMR spectrometers provide no means to do so, with the exception of varying the cable length and probe tuning.[5,6]

There have been different strategies employed to optimize NMR pulse sequences, e.g., by numerical optimization of the pulse sequence on a target spin system often in the form of optimum control.[11] Such an optimization can include the basic characteristics of the resonance circuit in the form of the transfer function[12,13] but this time-consuming approach needs to be repeated, ideally, for each sample and temperature as changing the experimental conditions changes the transfer function. Another approach is the direct optimization of pulse sequences on the spectrometer which also takes the characteristic of the resonance circuit into account.[14,15] A related approach which has specifically been used to suppress effects of phase transients is the experimental optimization of pulse sequence parameters that can partially counteract them[5,16] using a grid search. In all these approaches the obtained optimized pulse sequences will be specific to the transfer function of the experimental setup and must be reoptimized if the experimental setup or the tuning and matching changes. In the latter two cases, the optimization should take place on the sample to be studied which is challenging for biomolecules with limited signal-to-noise ratio. As an approximation, a test sample with sufficient signal-to-noise could be used. However, changing the sample will change the transfer function.

Our approach to transient compensation avoids these difficulties using a "digital tune up" of the spectrometer that requires no observable signal from the sample. This is achieved by modifying the input signal applied to the NMR probe such that the B_1 field actually seen by the spins closely mimics a "hard" rectangular pulse. In finite-bandwidth systems, like a tuned and matched NMR probe, achieving a perfect rectangular pulse is, however, impossible and we settle for a pulse with slightly rounded edges (finite rise time) but no out-of-phase contributions (Figure 1 C). This modification alone will not significantly change the phase transients (Figure 1 D), but we need to apply a pulse modified in phase and amplitude to obtain the desired B_1 field as shown in Figure 1 E and F. This approach is based on the results from previous work[12,17,18] where it was shown that such transient-compensated pulses give almost ideal nutation spectra.

Here we take transient compensation one step further and use transient-compensated pulses to implement windowless pulse sequences. In our approach, the performance of the pulse sequence is shown to be largely independent of the details of the experimental setup (vide infra). This spectrometer-dependent part enters the corrections to the input pulse shape needed to obtain transient-compensated radio-frequency pulses and is part of the spectrometer calibration procedure. Since pulses with rounded edges must be

[*] J. J. Wittmann, Prof. Dr. B. H. Meier, Prof. Dr. M. Ernst
Physical Chemistry, ETH Zürich
Vladimir-Prelog Weg 2, 8093 Zürich (Switzerland)
E-mail: beme@ethz.ch
maer@ethz.ch

Dr. K. Takeda
Division of Chemistry, Graduate School of Science, Kyoto University
606-8502 Kyoto (Japan)

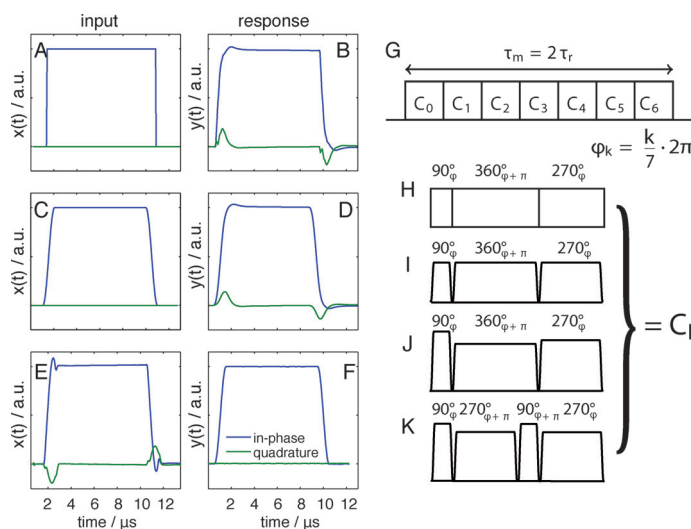Supporting information for this article is available on the WWW under http://dx.doi.org/10.1002/anie.201504782.

Figure 1. A) Rectangular excitation and B) typical response of the system under study. The transient behavior of the tuned resonator gives rise to an exponential build-up and decay as well as 90° phase-shifted components at the beginning and the end of the pulse. The in-phase component is drawn in blue, the out-of-phase component in green. These features are also observed in (D); the response towards an input shape with sine-shaped edges is shown in (C). E) In-phase and quadrature components of a transient-compensated input shape leads to a response (F) which is in good agreement to the target shape. G) C7 pulse sequence H) POST element with ideal rectangular pulses. I–K) Basic elements with finite rise-time pulses.

employed, pulse sequences must be slightly modified for optimum performance as detailed below.

We denote the B_1 field seen by the spins as $y(t)$ and the rf input given to the tuned circuit (probe) as $x(t)$. We can calculate the required input signal $x(t)$ (e.g., the one shown in Figure 1 E) needed to obtain the desired response $y(t)$ (Figure 1 F) in the framework of linear-response theory.[12,17,18] There, $y(t)$ is given by the convolution of $x(t)$ with the impulse-response function $h(t)$ [Eq. (1)].

$$y(t) = x(t) * h(t) = \mathscr{F}^{-1}\{\mathscr{F}\{x(t)\}\mathscr{F}\{h(t)\}\} \qquad (1)$$

Here, $h(t)$ describes the influence of all the elements of the rf circuit, such as probe, amplifiers, filters, and cables. $\mathscr{F}$ denotes the Fourier transform, $*$ the convolution integral. If one knows $h(t)$, a de-convolution allows the calculation of the input waveform that results in the target waveform [Eq. (2)].

$$x(t) = \mathscr{F}^{-1}\left\{ \frac{\mathscr{F}\{y(t)\}}{\mathscr{F}\{h(t)\}} \right\} \qquad (2)$$

To measure the actual rf field in the coil, $y(t)$, a pickup coil was placed close to the NMR coil. Among the several ways of experimentally characterizing the impulse-response function of the system $h(t)$, we decided to use maximum-length sequences (MLS)[12,19,20] (see the Experimental Section).

To evaluate the performance of transient-compensated pulse sequences we investigate the excitation of double-quantum coherence in solid-state NMR spectroscopy, which is known as a demanding and difficult to reproduce experiment, using the POST-C7 pulse sequence[21,22] shown in Figure 1 G.

To make the POST-C7 sequence more stable and efficient, several modifications have been proposed in the past. An adiabatic implementation of CN sequence has been proposed where the phase shift is varied to achieve a sweep through the resonance condition.[23] To compensate pulse transients, a phase shift of the first pulse of the POST element was proposed.[5] Finally, an asynchronous implementation of the POST-C7 sequence was shown to better compensate second-order effects from CSA tensors.[24]

In the POST-C7 pulse sequence, the rf irradiation is applied continuously and only the rf phase changes during the pulse sequence. Still the same criteria as for rectangular pulses apply and a compensation of the phase transients is possible as shown in Figure S1 in the Supporting Information. The Hamiltonian under an ideal C7 pulse sequence consists of the dipolar double-quantum term only [Eq. (3)], where κ is a complex scaling factor.

$$\bar{\mathscr{H}}_{\mathrm{D}} = \frac{1}{2}\omega_{1,2}\kappa[I_1^+I_2^+] + \frac{1}{2}\omega_{1,2}\kappa^*[I_1^-I_2^-] \qquad (3)$$

It can be shown[25] that in a first-order approximation the most important error terms are proportional to the chemical-shift interaction and have the form shown in Equation (4)

$$\bar{\mathscr{H}}_{\mathrm{err}} = \sum \varepsilon_i \omega_i I_{iz} \qquad (4)$$

with $i = 1,2$. For optimal results from the pulse sequence, the values of ε_1 and ε_2 have to be minimized while $|\kappa|$ is maximized. For an ideal C7 pulse sequence with rectangular pulses applied on resonance, $\varepsilon_1 = \varepsilon_2 = 0$ and $|\kappa| = 0.232$.[22] As mentioned above, the edges of the pulses must be rounded to be practical. In order to quantify the efficiency of the recoupling sequence, ε_i and $|\kappa|$ are calculated based on the Floquet description of symmetry-based sequences[25,24] as a function of the rise/fall time of the pulses, τ_{edge}, and the deviation of the rf-field amplitude ν_1 for the POST element from the nominal value (see Figure 2 A). A more detailed account of the Floquet approach for the case of amplitude-shaped pulses will be given elsewhere. In the limit of hard pulses (Figure 2 A, $\tau_{\mathrm{edge}} = 0$ μs) and using an ideal rf-field amplitude, a pure double-quantum Hamiltonian is obtained as the chemical-shift scaling factors ε_1 and ε_2 vanish. As seen from Figure 2 A, the double-quantum scaling factors, however, rapidly decrease to very small values with increasing τ_{edge}. For all practically realizable values of τ_{edge}, typically 0.5 to 1 μs, $|\kappa| \approx 0$ and no double-quantum excitation is predicted. The main reason is that due to the shaped amplitudes and the different length of the three pulses contained in the POST element, the net rotation over the C element is no longer zero and the C7 resonance condition is violated. To restore efficient double-quantum recoupling under rotor-synchronized rf irradiation, the basic C element has to be modified such that it corresponds again to a unity propagator without effective field. This can be realized by modifying the rf-field amplitude of the individual pulses such that the flip angles of each pulse in the basic element correspond again to
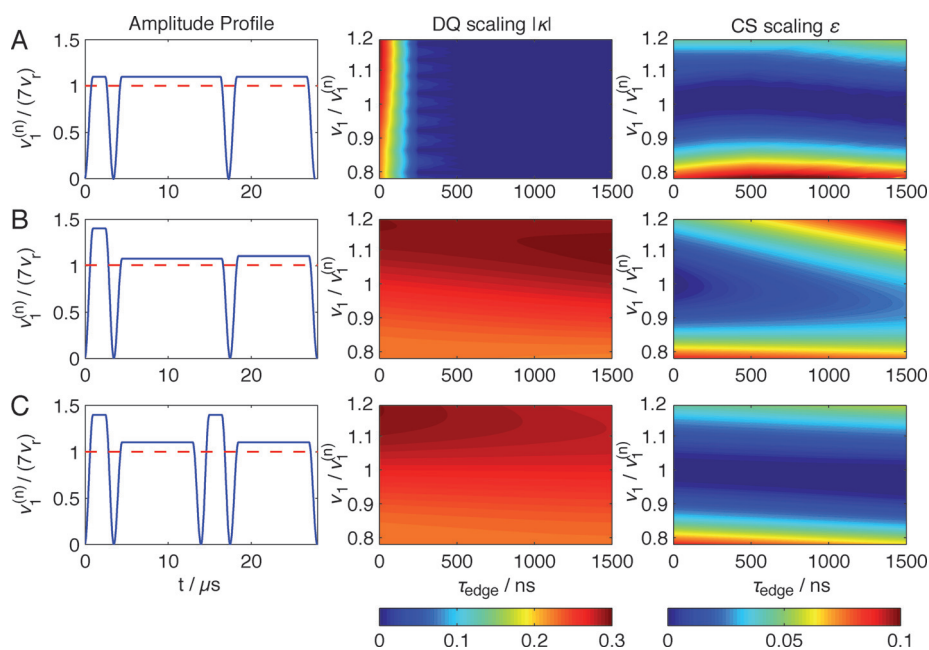
Figure 2. Dipolar and chemical-shift scaling factors, $|\kappa|$ and ε, as a function of the rise/fall time of the pulses (implemented as half a period of a sine function with duration τ_{edge}) and of the rf amplitude ν_1. The nominal rf-field amplitude $\nu_1^{(a)}$ with an average rf-field amplitude value of seven times the spinning frequency (e.g. 71.4 kHz at 10.2 kHz MAS) is shown in the first column for A) POST-C7, B) the amplitude-shaped and flip-angle-corrected POST-C7 that restores a unity propagator over one cycle and C) TIPTOP-C7.

with ^{13}C labels at the two carbonyl groups diluted 1:7 in natural-abundance material to minimize intermolecular contacts. Besides the small chemical-shift difference of the two carbonyl resonances (5.9 ppm), a rather large CSA tensor ($\delta = 77$ ppm and $\eta = 0.68$) competes with the recoupling of the dipolar interaction of $\nu_{12} = 585$ Hz corresponding to a distance of 0.296 nm.[27] Due to the smaller dipole coupling, this sample represents a more difficult case for recoupling. To emulate typical differences between spectrometers or between settings in different experimental sessions, we used three cables of different lengths between preamplifier and probe. The cable length significantly changes the properties of the resonance circuit because input impedance of the probe, cable impedance, and output impedance of the amplifier all do not perfectly match the nominal impedance of 50 Ω. The
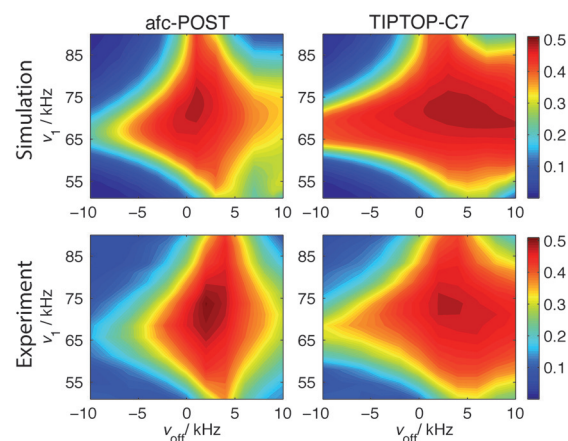
the nominal value in the ideal rectangular-pulse version as shown in Figure 2 B. Even though high double-quantum scaling factors are observed, the condition for optimal chemical-shift suppression narrows down considerably with increasing edge times and ε_i becomes non-zero (see Figure 2 B). This issue can be addressed by splitting the central 2π pulse into pulses of flip angles $3\pi/2$ and $\pi/2$. In this case (Figure 2 C), the internal symmetry of the basic element[26] is retained and, independent of τ_{edge}, a condition can be found with high $|\kappa|$ and $\varepsilon_1 \approx \varepsilon_2 \approx 0$. Thus, the modified basic element shown in Figure 2 C, which we designate TIPTOP (TIP angle and transient-optimized pulse) is therefore expected to show the best performance for amplitude-shaped composite pulses.

The properties of the TIPTOP-C7 DQ recoupling sequence were experimentally characterized using 1,2-$^{13}C_2$-glycine as a test sample. Both numerical simulations in a two-spin system and the experimental data (Figure 3) are in good agreement and consistent with the Floquet calculations (see Figure 2). The plots in Figure 3 show the polarization-transfer efficiency from the C′ to the Cα resonance as a function of the rf-field amplitude and the rf-carrier frequency. The zero point corresponds to the carrier set in the center between the two resonances. The pulse rise and fall time was set to 1 µs, a practically feasible value. Indeed, the corrected pulse sequences perform well, and the experimental values for the transfer efficiency and rf-amplitude and offset dependence are as predicted.

To further experimentally characterize the performance of the transient-compensated TIPTOP-C7 sequence, we chose a sample of doubly ^{13}C-labeled diammonium phthalate

Figure 3. Simulations and measurements are in accordance for all pulse sequences. Simulated and measured DQ transfer in $^{13}C_2$-glycine for the pulse sequences of Figure 2 B,C. For the simulations a monoexponential damping with a time constant of 16 ms, derived from the experimental data, was applied.

corresponding responses to a square pulse input function are given in Figure S2C–E. The maximum double-quantum transfer is achieved for a different value of ν_1, for each of the three cable lengths (Figure S2A), while the compensated pulses lead to an almost ideal and cable-length-independent transfer (Figure S2B). Correspondingly, the experimental POST-C7 double-quantum build-up, measured at the experimentally optimized value of ν_1, is far from the expected theoretical curve and depends strongly on the exact cable length
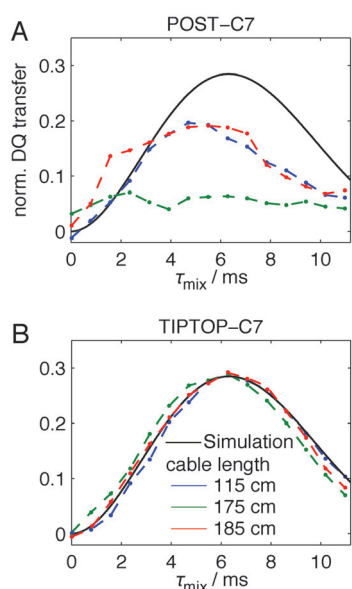
Figure 4. The compensated pulse sequence leads to significantly better results. Build-up of double-quantum coherence in diammonium phthalate (labeled at the carboxyl carbons) for three different cable lengths (blue 115 cm, green 175 cm, and red 185 cm) for the uncompensated POST-C7 pulse sequence (A) and for TIPTOP-C7 (B). The black line is the theoretical curve based on the internuclear distance from the crystal structure. Mono-exponential damping with a time constant of 11 ms, derived from the experimental data, was applied to the simulations.

(Figure 4 A). This behavior illustrates the experimental problems in implementing the double-quantum transfer. The situation is dramatically improved for the TIPTOP-C7 sequence using compensated pulses: the observed time dependence and maximum amplitude of the double-quantum build-up is almost identical to the theoretical expectation and is independent of the cable length (Figure 4 B).

In summary, we have demonstrated that the amplitude and phase of the rf field inside the NMR coil can be controlled to a high extent. Due to the finite rise and fall times of the compensated pulses, the flip angles of the individual pulses need to be corrected to obtain a unity propagator over a single C element. Implementing these modifications, we have found that transient-compensated symmetry-based recoupling leads to high recoupling efficiencies using the TIPTOP-C7 sequence and to a much higher reproducibility of the experiments, independent of the details of the experimental setup. In contrast to previous approaches, the transient-compensated pulses do not rely on an experimental optimization of the signal, which is difficult to achieve in samples with a low signal-to-noise ratio.

We are confident that this technical improvement will significantly improve our ability to coherently and consistently control the spin dynamics in a wide range of NMR experiments. Pulse sequences, already existing and novel ones, that were limited by their sensitivity to phase transients may now show improved behavior. This opens up new options in pulse-sequence design.

Experimental Section

$1,2\text{-}^{13}C_2$-glycine was purchased from Cambridge Isotopes and used without further purification. Phthalic acid-$2,2\text{-}^{13}C_2$ was purchased from Isotec and mixed with unlabeled phthalic acid in a molar ratio of 1:7. In order to reduce T_1 relaxation times, the diammonium salt was synthesized by adding an excess of aqueous ammonia. The product was obtained as a white crystalline powder after the solvent had been removed by lyophilization.

All experiments were carried out on a 400 MHz Bruker Avance III spectrometer with extended pulse-shape memory. The corresponding ^{13}C Larmor frequency was 100.63 MHz. Before the experiments were carried out, a standard Bruker 2.5 mm double-resonance probe was tuned to a minimum of the reflected power on both ^1H and ^{13}C channels. In order to measure the phase and amplitude of the B_1 field generated by the pulse, a pick-up coil was placed in close proximity to the NMR coil. The induced current (coupling -44 dB) was digitized with a sampling rate of 5 Gsample/s using a Tektronix TDS7104 oscilloscope. The impulse response function $h(t)$ was determined by measuring the response from the pickup coil $y(t)$ using a maximum-length-sequence MLS-8[20] with a time step per bit of 50 ns and a total length of 12.75 µs. Input, output, and the determined impulse response for one experimental setup are shown in Figure S3.

After digital quadrature demodulation of the signal followed by digital filtering, the pulse envelopes were obtained with a time resolution of 50 ns. Compensated pulse shapes were calculated and saved as Bruker shape files using the highest possible time resolution (50 ns) that could be sustained over the full mixing sequence (about 10 ms) using the extended pulse-shape memory. Digital signal processing was performed in MATLAB.[28]

Numerical simulations were performed using the GAMMA spin-simulation environment[29] using a set of 538 ZCW crystallite orientations.[30] The MAS frequency was set to 10.204 kHz for all simulations, Floquet calculations, and experiments. Orientations of dipole–dipole and chemical-shift tensors were extracted from quantum-chemical calculations based on the crystal structure.[27] Continuous-wave (cw) ^1H decoupling ($\nu_1 = 155$ kHz) was applied during the recoupling period.

[1] M. Mehring, *Rev. Sci. Instrum.* **1972**, *43*, 649.
[2] J. D. Ellett, M. G. Gibby, U. Haeberlen, L. M. Huber, M. Mehring, A. Pines, J. S. Waugh, *Adv. Magn. Reson* **1971**, *662*, 117–176.
[3] T. M. Barbara, J. F. Martin, J. Wurl, *J. Magn. Reson.* **1991**, *93*, 497–508.
[4] A. J. Vega, *J. Magn. Reson.* **2004**, *170*, 22–41.
[5] J. Weber, M. Seemann, J. Schmedt auf der Günne, *Solid State Nucl. Magn. Reson.* **2012**, *43–44*, 42–50.

[6] M. Carravetta, M. Edén, O. G. Johannessen, H. Luthman, P. J. Verdegem, J. Lugtenburg, A. Sebald, M. H. Levitt, *J. Am. Chem. Soc.* **2001**, *123*, 10628–10638.

[7] R. W. Vaughan, D. D. Elleman, L. M. Stacey, W.-K. Rhim, J. W. Lee, *Rev. Sci. Instrum.* **1972**, *43*, 1356.

[8] W.-K. Rhim, D. D. Elleman, R. W. Vaughan, *J. Chem. Phys.* **1973**, *59*, 3740.

[9] W.-K. Rhim, D. D. Elleman, L. B. Schreiber, R. W. Vaughan, *J. Chem. Phys.* **1974**, *60*, 4595.

[10] D. Burum, M. Under, R. R. Ernst, *J. Magn. Reson.* **1981**, *43*, 463–471.

[11] Z. Tošner, T. Vosegaard, C. Kehlet, N. Khaneja, S. J. Glaser, N. C. Nielsen, *J. Magn. Reson.* **2009**, *197*, 120–134.

[12] P. E. Spindler, Y. Zhang, B. Endeward, N. Gershernzon, T. E. Skinner, S. J. Glaser, T. F. Prisner, *J. Magn. Reson.* **2012**, *218*, 49–58.

[13] T. W. Borneman, D. G. Cory, *J. Magn. Reson.* **2012**, *225*, 120–129.

[14] B. Elena, G. de Paëpe, L. Emsley, *Chem. Phys. Lett.* **2004**, *398*, 532–538.

[15] D. L. A. G. Grimminck, S. K. Vasa, W. L. Meerts, A. P. M. Kentgens, A. Brinkmann, *Chem. Phys. Lett.* **2011**, *509*, 186–191.

[16] M. E. Halse, J. Schlagnitweit, L. Emsley, *Isr. J. Chem.* **2014**, *54*, 136–146.

[17] K. Takeda, Y. Tabuchi, M. Negoro, M. Kitagawa, *J. Magn. Reson.* **2009**, *197*, 242–244.

[18] Y. Tabuchi, M. Negoro, K. Takeda, M. Kitagawa, *J. Magn. Reson.* **2010**, *204*, 327–332.

[19] *Handbook of Signal Processing in Acoustics* (Eds.: D. Havelock, S. Kuwano, M. Vorländer), Springer, New York, **2008**.

[20] D. D. Rife, J. Vanderkooy, *J. Audio Eng. Soc.* **1989**, *37*, 419.

[21] M. H. Levitt, *J. Chem. Phys.* **2008**, *128*, 052205.

[22] M. Hohwy, H. J. Jakobsen, M. Edén, M. H. Levitt, N. C. Nielsen, M. Eden, *J. Chem. Phys.* **1998**, *108*, 2686.

[23] R. Verel, B. H. Meier, *ChemPhysChem* **2004**, *5*, 851–862.

[24] K. O. Tan, M. Rajeswari, P. K. Madhu, M. Ernst, *J. Chem. Phys.* **2015**, *142*, 065101.

[25] I. Scholz, J. D. van Beek, M. Ernst, *Solid State Nucl. Magn. Reson.* **2010**, *37*, 39–59.

[26] F.-C. Chou, H.-K. Lee, J. C. C. Chan, *J. Chem. Phys.* **2010**, *133*, 114503.

[27] R. A. Smith, *Acta Crystallogr. Sect. B* **1975**, *31*, 1773–1775.

[28] MATLAB The MathWorks Inc. Natick Massachusetts, **2012**.

[29] S. Smith, T. Levante, B. Meier, R. Ernst, *J. Magn. Reson.* **1994**, *106*, 75–105.

[30] V. B. Cheng, H. H. Suzukawa, M. Wolfsberg, *J. Chem. Phys.* **1973**, *59*, 3992.